Multinuclear Magnetic Resonance Spectroscopy Studies of the Structuration of the Tunnels of Sepiolite in the Presence of Intracrystalline Pyridine Molecules

Glenn A. Facey, Wenxing Kuang, and Christian Detellier*

Center for Research and Innovation in Catalysis and Department of Chemistry, University of Ottawa, Ottawa (Ontario), Canada K1N6N5

Received: July 12, 2005; In Final Form: September 25, 2005

Sepiolite, a naturally occurring magnesiosilicate nanoporous clay mineral with a tunnel structure, contains two types of water molecules in the structure: zeolitic water trapped inside the tunnels and structural water molecules which interact strongly with magnesium cations. The zeolitic water was removed by heating the sepiolite to 120 °C. The partially dehydrated sepiolite absorbed pyridine vapor to produce an intercalated material where the pyridine takes the place of the zeolitic water. ^{1}H solid-state MAS NMR spectroscopy showed that there is isotopic H/D exchange between pyridine-d_5 and the remaining structural water molecules of the sepiolite framework. The exchange takes place at room temperature over several days. Wide line solid state ^{2}H NMR of the sequestered pyridine-d_5 showed that two populations of pyridine molecules coexist in the material: one very mobile physisorbed population, which can be removed by heating at 90 °C, and a population due to pyridine trapped in the tunnels. Except for small in-plane librations, the trapped pyridine was shown to be held rigidly by the sepiolite. When the pyridine intercalated material is heated at 400 °C the structural water and some of the pyridine is lost. The remaining pyridine takes the place of the structural water to produce a new inorganic−organic nanohybrid material with the pyridine bound to the terminal Mg(II) in the structure. The pyridine in this material as well as the intercalated material was characterized by slow-spinning ^{15}N and ^{13}C CP/MAS NMR spectroscopy. The ^{15}N NMR was shown to be a very sensitive probe to characterize the various types of pyridine. The data indicate that pyridine molecules in the inorganic−organic nanohybrid material are directly bound to magnesium cations exposed in the tunnels of sepiolite.

Introduction

Sepiolite is a hydrated magnesiosilicate mineral characterized by a particular crystal structure, microfibrous morphology.[1] It has the ability to adsorb molecular, ionic, and polymeric species.[2−4] Sepiolite and palygorskite are minerals with similar structure and have been exploited for many applications, including their use by the Mayas to prepare a blue pigment (Maya Blue).[4] It was shown that sepiolite could be used to make membranes suitable for ultrafiltration,[5] or, with zeolites, for gas separation.[6] Sepiolite could also be used as an adsorbant,[7] a catalyst or catalyst carrier,[8] or as a template for the formation of carbon nanofibers.[9]

The theoretical half-unit-cell formula of sepiolite is $Si_{12}O_{30}$-$Mg_8(OH,F)_4(OH_2)_4 \cdot 8H_2O$.[10] The structure of sepiolite is derived from talc-like T−O−T ribbons that expand along the *c* direction, with a width of three pyroxene chains (Scheme 1). Each ribbon is connected to the next through an inverted Si−O−Si bond, resulting in a staggered talc layer with a continuous tetrahedral sheet and a discontinuous octahedral sheet. The discontinuous nature of the octahedral sheet allows for the formation of rectangular, tunnel-like micropores, which run parallel to the fiber axis and which are filled completely by zeolitic water $[H_2O]_{zeol}$ under ambient conditions. These nanostructured tunnels measure approximately 3.7 × 10.6 Å^2 in cross section, and they account in large part for the high specific surface area and excellent sorptive properties of sepiolite, once the zeolitic water has been removed by thermal treatment that does not exceed 150 °C. Small polar molecules, such as ammonia, methanol, ethanol, or acetone, can access the tunnels of sepiolite or palygorskite, either by displacing the zeolitic water molecules or by filling the free space after the previous removal of the latter by heating or by application of dynamic vacuum.[2−4] Finally, the terminal Mg(II), located at the edges of the

SCHEME 1

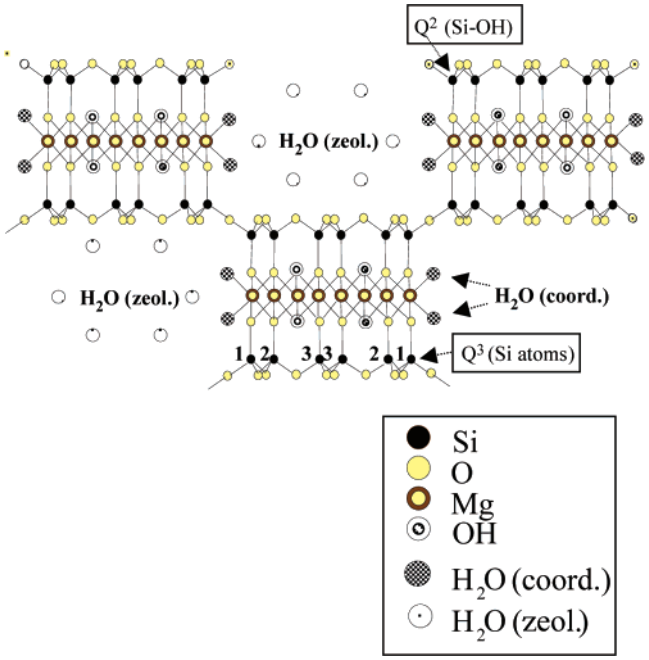

* To whom correspondence should be addressed. E-mail: dete@science.uottawa.ca. Phone: 613-562-5985. Fax: 613-562-5193.

10.1021/jp053832y CCC: $30.25
Published on Web 11/04/2005

octahedral sheets, complete their coordination with two molecules of structural water $[H_2O]_{coord}$, which are in turn hydrogen bonded to zeolitic water molecules located within the nanopores of the magnesiosilicate (Scheme 1).

It was shown recently that pyridine molecules are sequestered in sepiolite up to 450 °C, while sepiolite is fully dehydrated.[3] Upon incorporation in the tunnels of sepiolite at room temperature, the pyridine molecules are H-bound to the structural, Mg(II)-coordinated, water molecules. Upon heating, approximately 50% of the pyridine is lost together with the coordinated water molecules at temperatures below 200 °C. This event is accompanied by coordination of the remaining pyridine molecules to the edge Mg(II) ions in the octahedral sheets, resulting in a material with a structure similar to that of the parent sepiolite, but with pyridine molecules coordinated to the Mg(II) edge cations instead of structural water molecules.[3]

To apprehend the adsorbent, separation, and catalytic properties of sepiolite, it is essential to study the host−guest dynamics and interactions of organic molecules inserted in this mineral. In this study, solid state ^{1}H, ^{2}H, ^{15}N, and ^{13}C NMR measurements of the various states of pyridine molecules incorporated in the tunnels or adsorbed on the external surfaces of sepiolite were carried out. This study confirms the structuration of the tunnels of sepiolite when organic molecules are trapped inside them. The ^{15}N chemical shielding tensor components confirm the direct coordination of the nitrogen of pyridine to the edge Mg(II) exposed in the tunnels, associated with the removal of the structural water molecules.

Experimental Section

Materials. Sepiolite (SepSp-1) from Valdemoro, Spain, was obtained from the Source Clays Repository of the Clay Minerals Society (Purdue University), with a chemical composition (%) of SiO_2 (52.9), MgO (23.6), Al_2O_3 (2.56), Fe_2O_3 (1.22), FeO (0.3), MnO (0.13), and K_2O (0.05). Mineralogical analysis by X-ray diffraction showed that the crude sepiolite contained traces of quartz and calcite.[11] The crude sepiolite was purified according to previously reported procedures.[5a] The particle size was selectively restricted by passing the sepiolite samples through a 100-mesh sieve.

Pyridine (>99.9%, HPLC grade) was obtained from Aldrich Chemical Co. Pyridine-^{15}N (≥99% ^{15}N) and pyridine-$^2H_5$ (≥99.5% ^{2}H) were obtained from C/D/N Isotopes Inc.

Preparation of the Samples. Typically, sepiolite samples were heated with a ramp rate of 1 °C min^{-1} to 120 °C and then kept at 120 °C for 20 h under air in a baffle furnace, to eliminate selectively the surface-bound water and zeolitic water from the nanoporous tunnels. The vials containing dried sepiolite were immediately transferred into capped bottles containing a few milliliters of pyridine (pyridine-^{15}N for the ^{15}N NMR experiments, and pyridine-$^2H_5$ for the broadline ^{2}H NMR experiments) and then kept in contact with the pyridine vapor at room temperature.

Nuclear Magnetic Resonance Spectroscopy. Solid state ^{1}H magic-angle spinning (MAS) nuclear magnetic resonance (NMR) spectra were recorded at 200.10 MHz, at room temperature on a Bruker ASX-200 spectrometer. The spinning rate was 6 kHz. The excitation pulse and recycle time were 3.5 μs ($\pi/2$ pulse) and 2 s (16 scans), respectively. The ^{1}H NMR signals were externally referenced to the $-CH_3$ resonance of acetone at 2.06 ppm, corresponding to tetramethylsilane (TMS) at 0 ppm.

The ^{2}H broadline NMR experiments were measured at room temperature on a Bruker ASX-200 spectrometer, operating at 30.72 MHz, using the quadrupolar echo pulse technique,[12] with ^{2}H 90° pulses of 2.7 μs and an interpulse delay of 35μs. Typically 1500 scans were collected with a 2 s recycle time.

Solid state ^{15}N CP/MAS NMR spectra were recorded at 50.69 MHz at room temperature on a Bruker Avance 500 spectrometer, with a spinning rate of 2.5 kHz. A ramped CP pulse sequence was used for all ^{15}N NMR cross polarization experiments. The recycle delay time was 2 s, and the proton 90° pulse was 4 μs. The contact time to allow the transfer of magnetization between protons and ^{15}N nuclei was 5 ms. The ^{15}N NMR signals were externally referenced to the ammonium resonance of ammonium nitrate ($^{15}NH_4$)(NO_3) at −356.4 ppm, corresponding to nitromethane (CH_3)($^{15}NO_3$) at 0 ppm.

Solid state ^{13}C CP/MAS NMR spectra were acquired at 125.75 MHz on a Bruker Avance 500 spectrometer, with a spinning rate of 4 kHz. A ramped CP pulse was used in all ^{13}C cross-polarization experiments. The recycle delay time was 2 s, and the proton 90° pulse was 4 μs. The contact time to allow the transfer of magnetization between protons and ^{13}C nuclei was 2 ms. The ^{13}C signals were externally referenced to the high-frequency signal of adamantane at 38.4 ppm, corresponding to tetramethylsilane (TMS) at 0 ppm.

The proton decoupled ^{13}C high-resolution spectrum of neat pyridine was measured on a Bruker AMX-500 spectrometer operating at 125.77 MHz, using TMS as a dilute internal standard. A 45° pulse was used and 8 scans collected. The acquisition time was 3 s. The magnet was shimmed by optimizing the ^{1}H free induction decay.

Results and Discussion

^{1}H MAS NMR Measurements. Sepiolite was dried at 120 °C for 20 h and then exposed to pyridine-d_5 vapor for varying lengths of time. The ^{1}H MAS NMR spectra were recorded and are shown in Figure 1. In Figure 1a is the spectrum of sepiolite before any treatment. It consists of two partially overlapping peaks with their associated spinning sidebands. The sharper low-frequency line that produces only a few spinning sidebands is attributed to the internal hydroxyl groups while the broader high-frequency line that produces numerous spinning sidebands is attributed to two overlapping resonances assigned to the zeolitic and the structural water molecules present in the tunnel and channel structures.[13] When the sample is heated at 120 °C for 20 h (Figure 1b) the zeolitic water is removed and the spectrum consists of the sharp −OH line and the broad higher frequency line seen as a shoulder particularly observable in the spinning sidebands. It is attributed to the structural water molecules. The dehydrated sepiolite was exposed to the perdeuterated pyridine vapor for periods ranging from 3 min to 9 days. The ^{1}H MAS NMR spectra are shown in Figure 1c−j. From ^{29}Si CP/MAS data, it has been shown previously[3] that significant amounts of pyridine are absorbed into the nanoporous tunnels after only 10 to 15 min. Since the pyridine used in this study was perdeuterated, one does not expect to see substantial pyridine ^{1}H resonances develop as a function of exposure time. After 27 h of exposure to pyridine-d_5 vapor significant ^{1}H NMR signal intensities are observed, due to the pyridine signals, between 6 and 9 ppm. These resonances are much larger than those expected from the 0.5% residual protons present in the perdeuterated pyridine reagent and much smaller than those observed for a similar sample with protonated pyridine.[3] The observed proton resonances arise from isotopic ^{1}H/^{2}H exchange with the protons of the structural water molecules, sepiolite playing plausibly a catalytic role.

Broadline ^{2}H NMR Measurements. ^{2}H is a spin $I = 1$ nucleus having three Zeeman states whose energies are perturbed

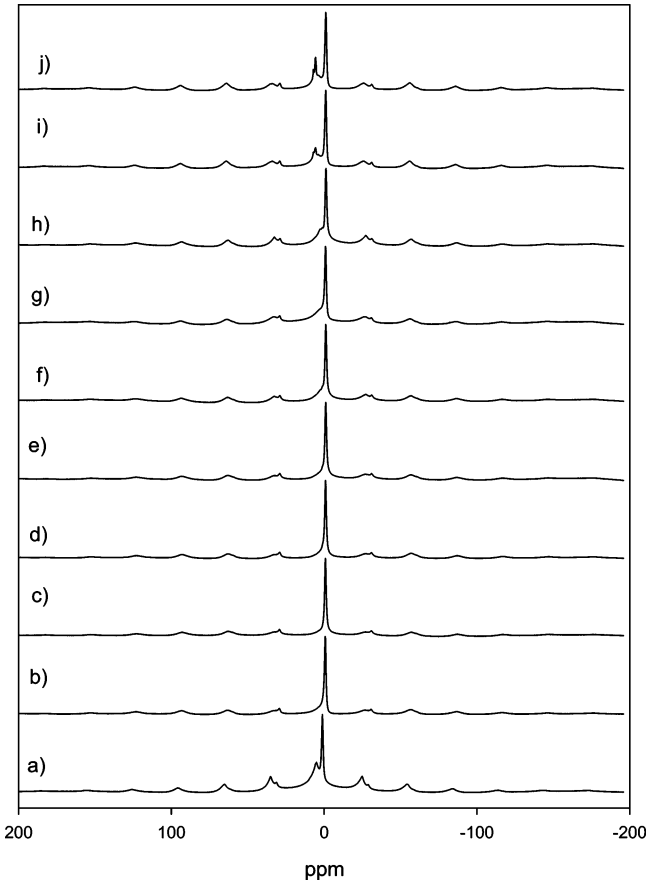

Figure 1. ^{1}H MAS NMR spectra of samples: (a) sepiolite; (b) sepiolite heated at 120 °C for 20 h; (c−j) sample b exposed to pyridine-d_5 for 1 min, 3 min, 7 min, 8.5 min, 10 min, 15 min, 27 h, and 9 days, respectively.

by the electric quadrupolar interaction. Each crystallographically unique deuteron has a pair of resonances with an energy difference dependent on the quadrupolar coupling constant $\chi = (e^2qQ/h)$, and the orientation of the electric field gradient at the nuclear site with respect to the magnetic field. The electric field gradient tensor, $\mathbf{V}_{ij}$, is usually very close to being axially symmetric about the C−D bonds of organic molecules, with its largest component, $V_{zz} = eq$, parallel to the bond. In powder samples all orientations of the C−D bonds with respect to the magnetic field are possible. This results in a powder pattern with three pairs of features given by:

$$\Delta\nu_{zz}=\nu_q \tag{1}$$

$$\Delta\nu_{yy}={}^1/_2\nu_q(1+\eta) \tag{2}$$

$$\Delta\nu_{xx}={}^1/_2\nu_q(1-\eta) \tag{3}$$

where $\nu_q = 3\chi/2$ and the asymmetry parameter $\eta = (\Delta\nu_{yy} - \Delta\nu_{xx})/\Delta\nu_{zz}$, where $0 \le \eta \le 1$ and $\Delta\nu_{xx} \le \Delta\nu_{yy} \le \Delta\nu_{zz}$ (see Figure 2). Also since $\mathbf{V}_{ij}$ is a traceless tensor, $\Delta\nu_{xx} + \Delta\nu_{yy} = \Delta\nu_{zz}$. When molecular motions occur on a time scale fast with respect to the quadrupolar interaction, components of the electric field gradient tensor are averaged thereby reducing the values of $\Delta\upsilon_{xx}$, $\Delta\upsilon_{yy}$, and $\Delta\upsilon_{zz}$. Isotropic motion will reduce all of the splittings to zero and yield an isotropic line whereas anisotropic motions will unequally average particular components of $\mathbf{V}_{ij}$, and may even leave one of the frequency separations unchanged with respect to the static spectrum.

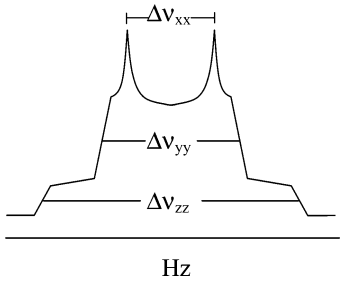

Figure 2. Calculated general ^{2}H NMR powder pattern with an asymmetry parameter of 0.2.

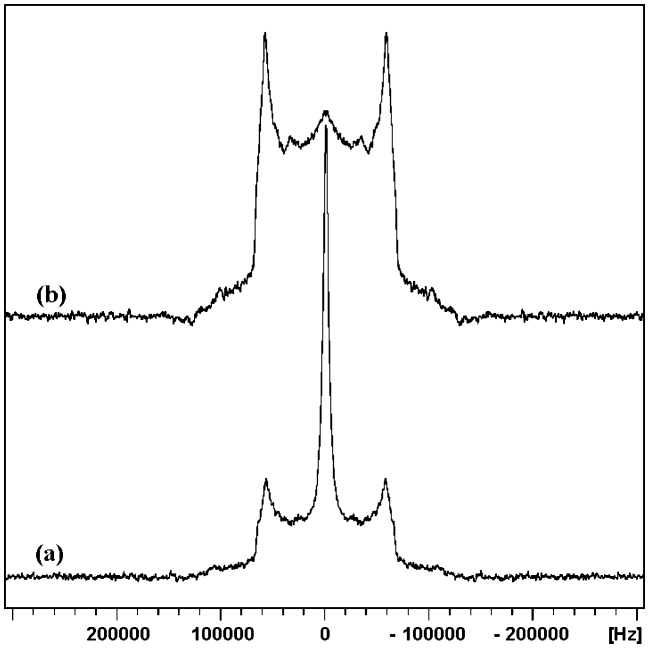

Figure 3. Broadline ^{2}H NMR spectra of the sepiolite heated at 120°C for 20 h, exposed to pyridine-d_5 vapor for a month, then heated at (a) 60 °C overnight and (b) 90 °C overnight.

The ^{2}H quadrupolar echo spectrum of dried sepiolite exposed to perdeuterated pyridine for one month and then heated at 60 °C overnight is shown in Figure 3a. The spectrum consists of an intense Lorentzian central line superposed on a much broader powder pattern at the base. The intense central peak is attributed to pyridine molecules adsorbed on the external surfaces undergoing rapid isotropic motion, while the broad powder pattern is predominantly attributed to pyridine molecules trapped inside the tunnels as well as some rigid structural HDO molecules from any isotopic exchange that may have occurred. Figure 3b shows the ^{2}H quadrupolar echo spectrum of the same sample heated to 90 °C overnight rather than at 60 °C. The spectrum shows predominantly the powder pattern, all the pyridine molecules adsorbed on external surfaces having been removed. It yields a quadrupolar coupling constant of $\chi = 168 \pm 2$ kHz and an asymmetry parameter of $\eta = 0.07 \pm 0.02$. These values indicate that there is a population of rigidly fixed pyridine molecules. The parameters compare reasonably well to those measured for solid pyridine at 77 K where pyridine was assumed to be rigid.[14] The data are summarized in Table 1. One can see from the data that $\Delta\upsilon_{yy}$ remains similar to that of solid pyridine whereas $\Delta\upsilon_{xx}$ and $\Delta\upsilon_{zz}$ are substantially reduced. It has been shown[14b] that $\Delta\upsilon_{yy}$ is proportional to the component of the electric field gradient tensor perpendicular to the plane of the pyridine ring while $\Delta\upsilon_{zz}$ and $\Delta\upsilon_{xx}$ are proportional to the components in the plane of the ring parallel and perpendicular to the C−D bonds, respectively. The reduction

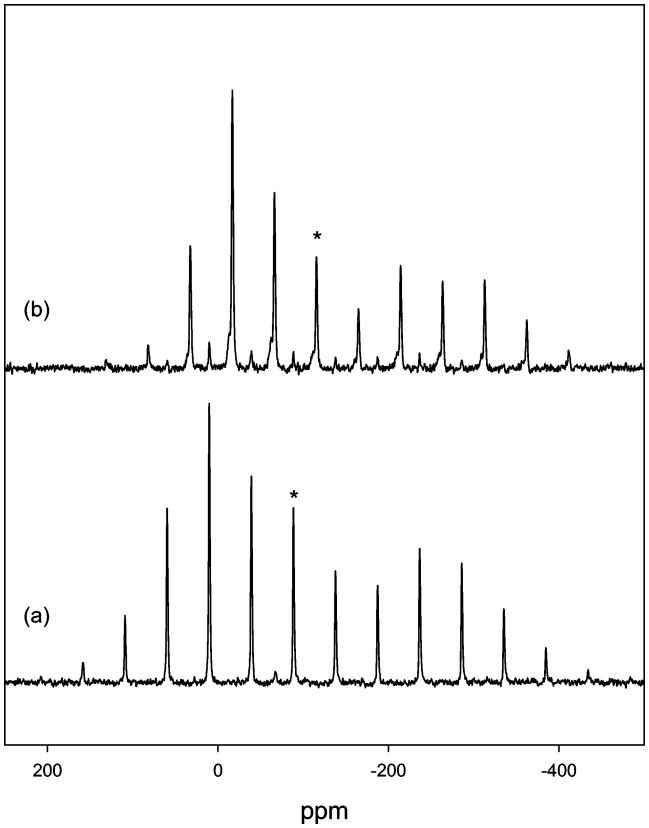

Figure 4. ^{15}N CP/MAS NMR spectra (spinning rate: 2.5 kHz) of sepiolite previously heated at 120 °C for 20 h, then exposed to pyridine-^{15}N (a) and heated to 400 °C (b).

TABLE 1: Comparison of the ^{2}H NMR Spectral Parameters for Pure Solid Pyridine Compared to Those for Sepiolite Heated at 120 °C for 20 H, Then Exposed to Pyridine-d_5 for a Month, and Finally Heated at 90 °C Overnight

	$\Delta\nu_{xx}$ (KHz)	$\Delta\nu_{yy}$ (KHz)	$\Delta\nu_{zz}$ (KHz)	η
this work (room temp)	117	135	252	0.07
ref 14b (77 K)	132	142	274	0.04
ref 14a	128	139	267	0.04

in both $\Delta\upsilon_{xx}$ and $\Delta\upsilon_{zz}$ compared to pure solid pyridine at 77 K indicates that the rings are undergoing a small-amplitude in-plane motion but are otherwise held quite rigidly. The in-plane motion leaves $\Delta\upsilon_{yy}$ unchanged.

^{15}N CP/MAS Measurements. ^{15}N chemical shifts have been shown to be very informative about the local environment of the nitrogen for pyridine in solution where, for example, chemical shift differences of approximately 20 ppm have been observed between neat pyridine and pyridine in water at infinite dilution.[15] Large chemical shift differences have also been observed for pyridine absorbed on different sites of alumina[16] and for pyridine absorbed into clay minerals.[17] The slow-spinning ^{15}N CP/MAS spectrum of sepiolite dried at 120 °C and exposed to ^{15}N-labeled pyridine for 20 h is shown in Figure 4a. The spectrum consists of an isotropic line at −88.7 ppm with sidebands spaced at the spinning speed of 2500 Hz, the intensities mimicking the ^{15}N chemical shielding tensor. This resonance can be attributed to pyridine adsorbed into the tunnels of sepiolite where it interacts with the structural water molecules. The isotropic chemical shift is similar to those measured for pyridine in other clay minerals[17] as well as for hydrated pyridine in solution. The much smaller peak at −67.2 ppm lacks spinning sidebands and can be attributed to mobile pyridine on the external surfaces of the clay. This liquidlike pyridine moves essentially isotropically and does not cross polarize very efficiently due to the motionally averaged dipolar coupling accounting for its very low intensity in the spectrum. It shows up much more clearly in the MAS spectrum[3] where the rapid isotropic motion does not attenuate the NMR signal. The chemical shift of the surface bound pyridine differs by only a few ppm from that of neat pyridine or physisorbed pyridine on alumina.[16a]

TABLE 2: ^{15}N Chemical Shielding Tensors of Sepiolite Heated at 120 °C for 20 h, Then Exposed to Pyridine-^{15}N for a Month[a]

	δ_{11} (ppm)	δ_{22} (ppm)	δ_{33} (ppm)	δ_{iso} (ppm)	Ω (ppm)	κ
without heating[b]	129.8	−7.2	−388.6	−88.7	518.4	0.472
heated at 400°C[b]	56.3	4.5	−408.1	−115.7	464.4	0.776
ref 22b[c]	200	33	−422	−63	622	0.463
ref 22a[d]	252.8	33.8	−529.2	−80.9	782.0	0.440

[a] All spectra were referenced to neat $CH_3{}^{15}NO_3$. [b] Taken at room temperature. [c] Taken at −100 °C. [d] Taken at −105 °C.

Figure 4b shows the ^{15}N CP/MAS spectrum of a sample of sepiolite dried at 120 °C, exposed to ^{15}N pyridine and then heated to 400 °C overnight. It was shown previously[3] that heating to 400 °C removes most of the structural water of sepiolite and some of the pyridine molecules. The spectrum shows a new peak at −115.7 ppm, 27 ppm more shielded than the absorbed pyridine in Figure 4a. This new resonance is attributed to pyridine coordinated directly to the edge Mg sites through the nitrogen.[3] The observed isotropic chemical shift is comparable to that of pyridine attached to the Lewis acid sites of alumina[16] or pyridine directly coordinated to cobalt in the cobaloxime, $pyCo(DH)_2CH_3$ where py = pyridine and DH = dimethylgloxime.[18] On close inspection of the resonance due to the Mg-coordinated nitrogen, one finds that it consists of a sharp peak and a much smaller broad complicated resonance slightly deshielded with respect to the larger resonance. Although a precise intensity ratio between the two resonances is difficult to obtain due to overlap, it was estimated in an NMR spectrum acquired at a much faster spinning rate to be approximately 9:1. The small feature may be due to nitrogen coordinated to the quadrupolar ^{25}Mg ($I = {}^5/_2$ natural abundance = 10%) whereas the larger narrower peak is due to nitrogen bound to ^{24}Mg and ^{26}Mg ($I = 0$ natural abundance = 79% and 11%, respectively), the chemical shift difference being due to an isotope effect. The shape of the broad resonance would be complicated by the dipolar coupling to the quadrupolar ^{25}Mg not completely averaged by magic-angle spinning as well as J coupling.[19] An alternative interpretation is that the smaller resonance may be due to nitrogen bound to less abundant metals in the structure, such as aluminum or iron.

The shielding tensors were calculated for each of the ^{15}N resonances by using the HBA program[20] employing the Hertzfeld−Berger method of spinning sideband analysis.[21] The chemical shielding parameters of the absorbed pyridine and the Mg-coordinated pyridine are given in Table 2 along with those reported for pure solid pyridine.[22] The reconstructed shielding tensors for the Mg-coordinated pyridine, the adsorbed pyridine, and pure solid pyridine are shown in Figure 5, lines a−c, respectively. It is apparent that the shielding tensors are quite different for each of the three cases. In the cases of both the neat pyridine and the adsorbed pyridine, the nitrogen atom is formally bound only to the two adjacent carbon atoms whereas in the case of the Mg-coordinated pyridine the nitrogen is also bound to the Mg Lewis acid sites of sepiolite. The ^{15}N shielding tensor for the adsorbed pyridine has a smaller span, Ω, but a

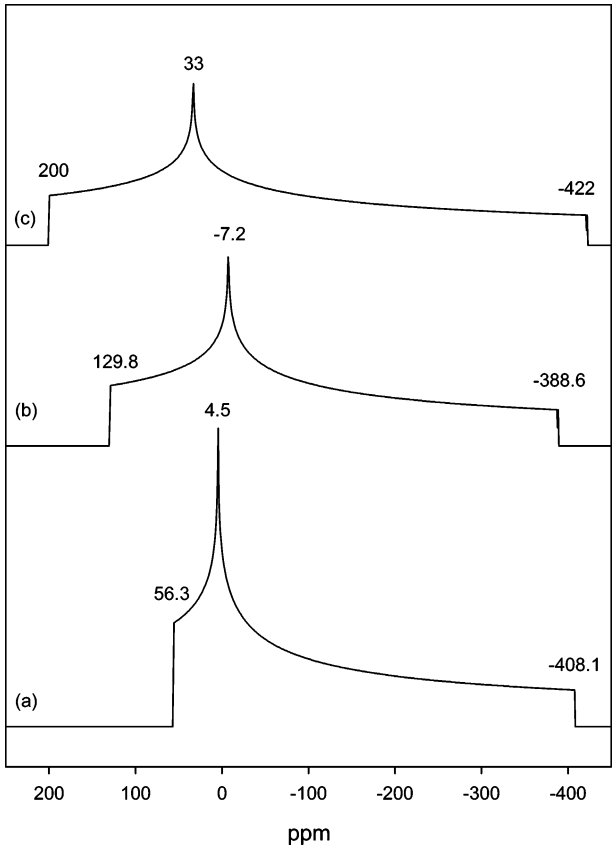

Figure 5. ^{15}N chemical shift tensors reconstructed from the Herzfeld−Berger analysis for pyridine-^{15}N, of sepiolite: (b) previously heated at 120 °C for 20 h, then exposed to pyridine-^{15}N (a) and heated to 400 °C and (c) pure solid pyridine (from ref 22b).

very similar skew, κ, compared to the pure pyridine. The shielding tensor for the Mg coordinated pyridine, however, is strikingly different. It has the smallest span of the three and the largest skew. For pure pyridine, the directions of the chemical shielding tensor components have been assigned as follows:[22b] $\delta_{11} = \delta_{tan}$ tangential to the C−N−C bond angle in the plane of the ring; the $\delta_{22} = \delta_{rad}$ bisecting the C−N−C bond angle radially in the plane of the ring, and the $\delta_{33} = \delta_{\perp}$ perpendicular to the ring plane. In the case of N-substituted pyridines[22b] and pyridine coordinated to cobalt[18] the most deshielded component, δ_{11}, equals δ_{rad} and $\delta_{22} = \delta_{tan}$ (i.e., reversed from that of pure pyridine), whereas the most shielded component, δ_{33}, remains as $\delta_{\perp}$. Since the Mg-coordinated pyridine is a substituted pyridine we can make the assumption that the most deshielded component, δ_{11}, equals δ_{rad} and that the δ_{rad} component becomes only 23.3 ppm more deshielded compared to that of pure pyridine while δ_{tan} and $\delta_{\perp}$ become 195.5 ppm more shielded and 13.9 ppm more deshielded, respectively. Although intuitively one may expect δ_{rad} to vary the most when comparing pure pyridine and Mg-coordinated pyridine, it is δ_{tan} that shows the greatest effect. This has been explained in terms of molecular orbital arguments and has been demonstrated both experimentally and theoretically.[18,22b]

^{13}C CP/MAS Spectra. Slow-spinning ^{13}C CP/MAS spectra were measured for samples of sepiolite previously heated to 120 °C for 20 h and exposed to pyridine, and then subsequently heated to 90 °C and heated overnight at 400 °C. The results are presented in Figure 6, parts a and b, respectively. The spectra consist of three isotropic lines representing the C2, C3, and C4 carbons of pyridine as well as the spinning sidebands mimicking the chemical shielding tensors for each of the carbons. The

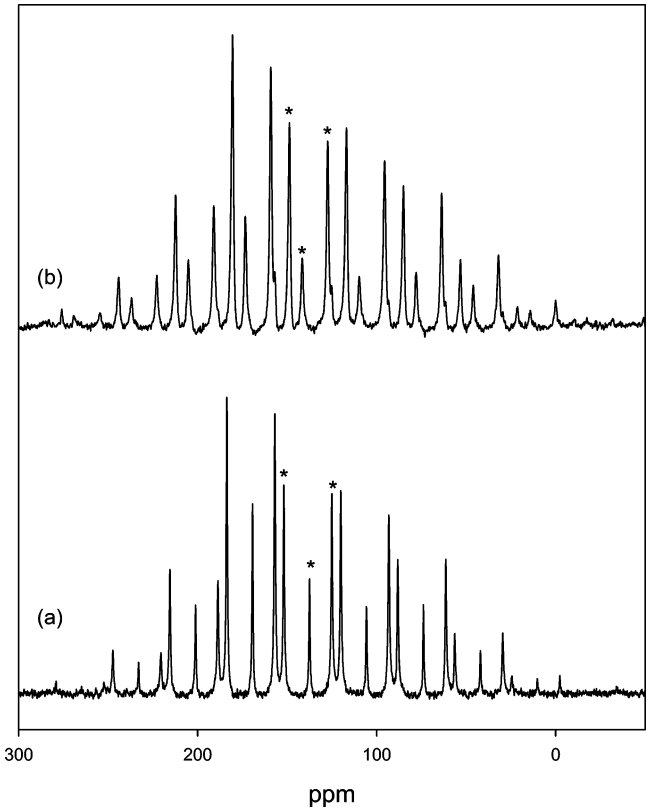

Figure 6. ^{13}C CP/MAS NMR spectra of sepiolite: (a) previously heated at 120 °C for 20 h, exposed to pyridine, then heated at 90°C overnight and (b) heated at 400 °C overnight.

spinning rates were chosen so as to ensure no overlap between isotropic lines and spinning sidebands. The C2, C3, and C4 resonances for the sample heated to 90 °C where pyridine is trapped in the nanotunnels and interacts with structural water appear at 151.8, 125.0, and 137.5 ppm, respectively. The spectrum acquired for the sample heated at 400 °C has three main isotropic peaks at 148.7, 127.3, and 141.6 ppm for the C2, C3, and C4 carbons, respectively. The spectrum also has a minor resonance as a low-frequency shoulder on the C3 peak. This is a residual resonance from the pyridine trapped in the nanotunnels interacting with structural water. In spectra acquired at higher spinning speeds, it is obvious that all three of the main resonances have similar shadow peaks. These values can be compared to those measured for neat liquid pyridine of 150.3, 124.0, and 136.0 ppm for the C2, C3, and C4 carbons, respectively. There is no more than 1.5 ppm difference between the values for the sample heated at 90 °C compared to those measured in solution. For the sample heated at 400 °C, the C3 and C4 carbons are 3.3 and 5.6 ppm more deshielded compared to those measured for the neat liquid.

The shielding tensors were calculated for each of the ^{13}C resonances by using the HBA program[20] employing the Hertzfeld−Berger method of spinning sideband analysis.[21] The chemical shielding parameters of the absorbed pyridine and the Mg-coordinated pyridine are given in Table 3 along with those reported for pyridine in a liquid crystalline solvent.[23] The reconstructed shielding tensors for the C3 carbon of the Mg-coordinated pyridine, the absorbed pyridine, and pyridine from ref 23 are shown in Figure 7. They are given as Supporting Information for C2 and C4 (Figures a and b). Unlike the ^{15}N shielding tensors which showed a large variability, the ^{13}C tensors are quite similar for all three types of pyridine.

TABLE 3: ^{13}C Chemical Shielding Tensors of Sepiolite Previously Heated at 120°C for 20 h, Then Exposed to Pyridine

		δ_{11} (ppm)	δ_{22} (ppm)	δ_{33} (ppm)	δ_{iso} (ppm)[a]	Ω (ppm)	κ
heated at 90 °C	C2	247	164	44	151.8	203	0.180
overnight	C3	218	140	18	125.0	200	0.225
	C4	232	162	18	137.5	214	0.343
heated at 400 °C	C2	247	161	38	148.7	209	0.177
overnight	C3	225	141	15	127.3	210	0.200
	C4	250	168	6	141.6	244	0.328
pyridine[b]	C2	241	173	35.5	149.8	205.5	0.339
	C3	205	158	7.5	123.5	197.5	0.524
	C4	233	170	4.4	135.8	228.6	0.449
neat liquid	C2				150.3		
pyridine	C3				124.0		
	C4				136.0		

[a] Measured from the CP/MAS spectra or the neat liquid. [b] Reference 23.

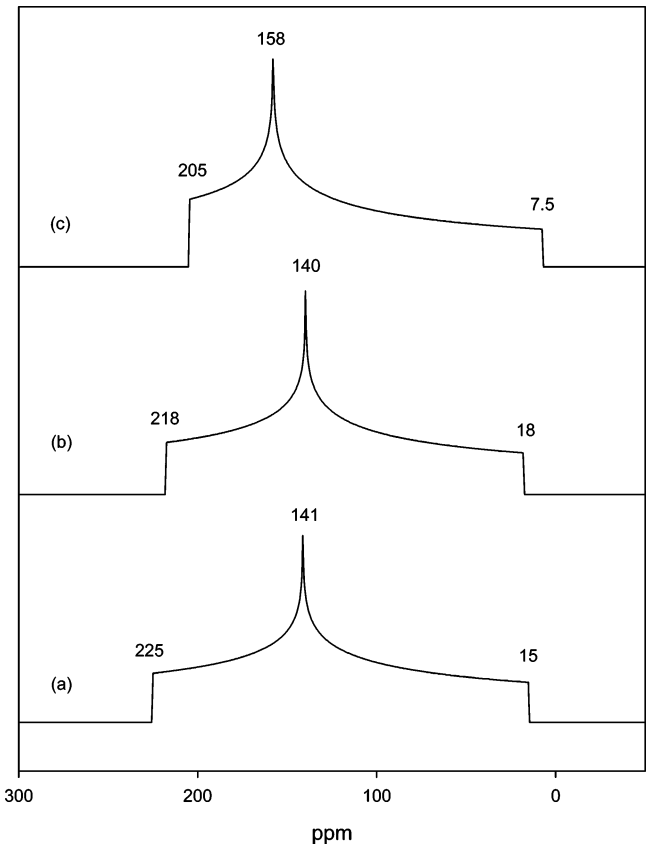

Figure 7. ^{13}C chemical shift tensors reconstructed from the Herzfeld−Berger analysis for pyridine (C3), of sepiolite previously heated at 120 °C for 20 h, exposed to pyridine, and (b) heated at 90 °C overnight, (a) heated at 400 °C overnight, and (c) pure pyridine (from ref 23).

Conclusion

Once the zeolitic water is removed from sepiolite, the mineral readily absorbs pyridine from the vapor phase. Broadline ^{2}H NMR measurements reveal that pyridine is adsorbed on external surfaces and is also trapped inside the nanotunnels. The surface pyridine is very mobile and can be removed by gentle heating at 90 °C. With the exception of a small-scale in-plane libration, the absorbed pyridine is held rigidly in the nanoporous tunnels of sepiolite where it is hydrogen bonded to the structural water molecules of the sepiolite. ^{1}H MAS NMR measurements showed that the absorbed pyridine undergoes isotopic ^{1}H/^{2}H exchange with the structural water molecules. When heated to 400 °C the structural water is entirely removed from the material along with some of the pyridine. The ^{15}N chemical shielding parameters show that the remaining pyridine molecules replace structural water, being coordinated directly through nitrogen to the edge magnesium cations.

This study confirms the structuration of the tunnels of sepiolite when organic molecules are trapped into them. The ^{15}N chemical shielding tensor components confirm the direct coordination of the nitrogen of pyridine to the edge Mg(II) exposed in the tunnels, associated with the removal of the structural water molecules. This study confirms also the successful design of highly structured organomineral nanohybrids, based on naturally occurring and abundant minerals, such as sepiolite.

Acknowledgment. The Natural Sciences and Engineering Research Council of Canada (NSERC) is gratefully acknowledged for a Discovery Grant.

Supporting Information Available: ^{13}C chemical shift tensors reconstructed from the Herzfeld−Berger analysis for pyridine C2 and C4. This material is available free of charge via the Internet at http://pubs.acs.org.

References and Notes

(1) Jones, B. F.; Galan, E. In R*eviews in Mineralogy;* Bailey, S. W., Ed.; Mineralogical Society of America: Washington, DC, 1988; Vol. 19, Hydrous Phyllosilicates; Chapter 16, Sepiolite and palygorskite; pp 631−674.

(2) (a) Barrer, R. M.; Mackenzie, N. *J. Phys. Chem.* **1954**, *58*, 560−568. (b) Serna, C.; Fernandez-Alvarez, T. *Anal. Quim.* **1974**, *70*, 760−764. (c) Inagaki, S.; Fukushima, Y.; Doi, H.; Kamigaito, O. *Clay Min.* **1990**, *25*, 99−105. (d) d'Espinose de la Caillerie, J.-B.; Gruver, V.; Fripiat, J. J. *J. Catal.* **1995**, *151*, 420−430 (e) Rytwo, G.; Nir, S.; Margulies, L.; Casal, B.; Merino, J.; Ruiz-Hitzky, E.; Serratosa, J. M. *Clays Clay Min.* **1998**, *46*, 340−348. (f) Shariatmadari, H.; Mermut, A. R.; Benke, M. B. *Clays Clay Min.* **1999**, *47*, 44−53 (g) Weir, M. R.; Facey, G. A.; Detellier, C. *Stud. Surf. Sci. Catal.* **2000**, *129*, 551−558. (h) Ruiz-Hitzky, E. *J. Mater. Chem.* **2001**, *11*, 86−91. (i) Rytwo, G.; Tropp, D.; Serban, C. *Appl. Clay Sci.* **2002**, *20*, 273−282. (j) Akyüz, S.; Akyüz, T. *J. Mol. Struct.* **2003**, *205*−*210*, 651−653. (k) Kuang, W.; Facey, G. A.; Detellier, C. *Clays Clay Min.* **2004**, *52*, 635−642 (l) Kuang, W.; Detellier, C. *Can. J. Chem.* **2004**, *82*, 1527−1535.

(3) Kuang, W.; Facey, G. A.; Detellier, C.; Casal, B.; Serratosa, J. M.; Ruiz-Hitzky, E. *Chem. Mater.* **2003**, *15*, 4956−4967.

(4) (a) Gettens, R. J. *Am. Antiq.* **1962**, *27*, 557−564. (b) Shepard, A. *Am. Antiq.* **1962**, *27*, 565−566. (c) Van Olphen, H. *Science* **1966**, *154*, 645−646. (d) Kleber, R.; Masschelein-Kleiner, L.; Thissen, J. *Stud. Conserv.* **1967**, *12*, 41−56. (e) Yacamán, M. J.; Rendon, L.; Arenas, J.; Puche, M. C. S. *Science* **1996**, *273*, 223−225. (f) Polette, L. A.; Meitzner, G.; Yacamán, M. J.; Chianelli, R. R. *Microchem. J.* **2002**, *71*, 167−174. (g) Hubbard, B.; Kuang, W.; Moser, A.; Facey, G. A.; Detellier, C. *Clays Clay Min.* **2003**, *51*, 318−326. (h) Fois, E.; Gamba, A.; Tilocca, A. *Microporous Mesoporous Mater.* **2003**, *57*, 263−272.

(5) (a) Weir, M. R.; Rutinduka, E.; Detellier, C.; Feng, C. Y.; Wang, Q. K.; Matsuura, T.; Le Van Mao, R. *J. Membr. Sci.* **2001**, *182*, 41−50. (b) Wang, Q. K.; Matsuura, T.; Feng, C. Y.; Weir, M. R.; Detellier, C.; Rutinduka, E.; Le Van Mao, R. *J. Membr. Sci.* **2001**, *184*, 153−163.

(6) Le Van Mao, R.; Rutinduka, E.; Detellier, C.; Gougay, P.; Hascoet, V.; Tavakoliyan, S.; Hoa, S. V.; Matsuura, T. *J. Mater. Chem.* **1999**, *9*, 783−788.

(7) (a) Casal, B.; Merino, J.; Serratosa, J. M.; Ruiz-Hitzky, E. *Appl. Clay Sci.* **2001**, *18*, 245−254. (b) Kara, M.; Yuzer, H.; Sabah, E.; Celik, M. S. *Water Res.* **2003**, *37*, 224−232.

(8) (a) Aramendía, M. A.; Borau, V.; Jiménez, C.; Marinas, J. M.; Porras, A.; Urbano, F. J.; Villar, L. *J. Mol. Catal.* **1994**, *94*, 131−147. (b) Damyanova, S.; Daza, L.; Fierro, J. L. G. *J. Catal.* **1996**, *159*, 150−161.

(9) (a) Sandi, G.; Winans, R. E.; Seifert, S.; Carrado, K. A. *Chem. Mater.* **2002**, *14*, 739−742. (b) Cheng, J. P.; Tu, J. P.; Ye, Y.; Sun, Y. L.; Liu, F.; Ning, Y. S.; Kong, F. Z.; Lu, H. M.; Zhang, X. B. *Chin. Chem. Lett.* **2002**, *13*, 381−384.

(10) (a) Preisinger, A. *Clays Clay Min.* **1959**, *6*, 61−67. (b) Santarén, J.; Sanz, J.; Ruiz-Hitzky, E. *Clays Clay Min.* **1990**, *38*, 63−68.

(11) Shuali, U.; Steinberg, M.; Yariv, S.; Müller-Vonmoos, M.; Kahr, G.; Rub, A. *Clay Min.* **1990**, *25*, 107−119.

(12) Davis, J. H.; Jeffrey, K. R.; Bloom, M.; Valic, M. I.; Higgs, T. P. *Chem. Phys. Lett.* **1976**, *42*, 390.

(13) (a) Aramendiá, M. A.; Jiménez, V. B. C.; Marinas, J. M.; Ruiz, J. R. *Solid State NMR* **1997**, *8*, 251−256. (b) Weir, M. R.; Kuang, W.; Facey, G. A.; Detellier, C. *Clays Clay Min*. **2002**, *50*, 240−247.
(14) (a) Barnes, R. G.; Bloom, J. W. *J. Chem. Phys*. **1972**, *57*, 3082. (b) Facey, G. A.; Ratcliffe, C. I.; Ripmeester, J. A. *J. Phys. Chem.* **1995**, *99*, 12249.
(15) Duthaler, R. O.; Roberts, J. D. *J. Am. Chem. Soc.* **1978**, *100*, 4969.
(16) (a) Ripmeester, J. A. *J. Am. Chem. Soc.* **1983**, *105*, 2925. (b) Majors, P. D.; Ellis, P. D. *J. Am. Chem. Soc.* **1987**, *109*, 1648.
(17) Ukrainczyk, L.; Smith, K. A. *Environ. Sci. Technol.* **1996**, *30*, 3167.
(18) Schurko, R. W.; Wasylishen, R. E. *J. Phys. Chem. A* **2000**, *104*, 3410.
(19) Harris, R. K.; Olivieri, A. C. *Prog. NMR Spectrosc*. **1992**, *24*, 435.
(20) Eichele, K. *HBA*, version 1.2, 1995.
(21) Herzfeld, J.; Berger, A. E. *J. Chem. Phys.* **1980**, *73*, 6021.
(22) (a) Schweitzer, D.; Spiess, H. W. *J. Magn. Reson.* **1974**, *15*, 529. (b) Solum, M. S.; Altmann, K. L.; Strohmeier, M.; Berges, D. A.; Zhang, Y.; Facelli, J. C.; Pugmire, R. J.; Grant, D. M. *J. Am. Chem. Soc*. **1997**, *119*, 9804.
(23) Parhami, P.; Fung, B. M. *J. Am. Chem. Soc.* **1985**, *107*, 7304.